PNAS RESEARCH ARTICLE | MICROBIOLOGY

Riding apoptotic bodies for cell–cell transmission by African swine fever virus

Peng Gao[a,1], Lei Zhou[a,1], Jiajun Wu[b,1], Wenlian Weng[a], Hua Wang[a], Miaomiao Ye[a], Yajin Qu[a], Yuxin Hao[b], Yongning Zhang[a], Xinna Ge[a], Xin Guo[a], Jun Han[a,2], and Hanchun Yang[a,2]

Edited by Bernard Moss, National Institute of Allergy and Infectious Diseases, Bethesda, MD; received June 7, 2023; accepted October 25, 2023

African swine fever virus (ASFV), a devastating pathogen to the worldwide swine industry, mainly targets macrophage/monocyte lineage, but how the virus enters host cells has remained unclear. Here, we report that ASFV utilizes apoptotic bodies (ApoBDs) for infection and cell–cell transmission. We show that ASFV induces cell apoptosis of primary porcine alveolar macrophages (PAMs) at the late stage of infection to productively shed ApoBDs that are subsequently swallowed by neighboring PAMs to initiate a secondary infection as evidenced by electron microscopy and live-cell imaging. Interestingly, the virions loaded within ApoBDs are exclusively single-enveloped particles that are devoid of the outer layer of membrane and represent a predominant form produced during late infection. The in vitro purified ApoBD vesicles are capable of mediating virus infection of naive PAMs, but the transmission can be significantly inhibited by blocking the "eat-me" signal phosphatidyserine on the surface of ApoBDs via Annexin V or the efferocytosis receptor TIM4 on the recipient PAMs via anti-TIM4 antibody, whereas overexpression of TIM4 enhances virus infection. The same treatment however did not affect the infection by intracellular viruses. Importantly, the swine sera to ASFV exert no effect on the ApoBD-mediated transmission but can partially act on the virions lacking the outer layer of membrane. Thus, ASFV has evolved to hijack a normal cellular pathway for cell–cell spread to evade host responses.

ASFV | cell to cell transmission | apoptotic bodies | immune evasion

Significance

ASFV is a leading threat to the world pork production and has evolved a mechanism to avoid antibody neutralization, contributing to viral persistence within infected pigs. We report here that ASFV highjacks the cellular efferocytosis pathway to ride the apoptotic bodies for cell–cell transmission of viral outer-membrane-free particles. The finding sheds light on the mechanisms of ASFV entry and transmission and also provides a means of viral immune evasion of antibodies.

African swine fever virus (ASFV) is an economically devastating pathogen to the world swine industry and represents a major threat to the world swine-producing regions. It was first reported in Africa in 1921 and then spread to Europe on three occasions during the past 100 y (1). In 2018, ASFV spread to China, the first country in Asia for ASF outbreaks and has since devastated the Chinese swine production, leading to colossal economic losses (2–4). Up to now, many countries in Africa, Europe, and Asia remain infected with ASFV (5–7). ASFV is a nucleocytoplasmic large DNA virus with a diameter around 200 nm that is wrapped by two layers of membranes separated by capsid and is the only member of the *Asfarviridae* family (8–10). Clinically, ASFV can cause high fever and systematic hemorrhage of wild and domestic pigs with a mortality rate up to 100% (11, 12). Currently, there are no effective vaccines or treatments available.

ASFV mainly infects cells of macrophage–monocyte lineage (13). The past studies have shown that this virus can use endocytosis and macropinocytosis for host entry (13–16), with much focusing on post-receptor binding stages, such as uncoating and membrane fusion, that involve a series of viral factors (e.g., E248R, E199L, B117L, etc.) (17–20), but the early entry events such as the receptor usage and binding have remained poorly understood. Antibodies are thought to play a role in control of ASFV infection, as passive transfer of colostrum or serum antibodies from convalescent pigs can result in reduced viremia and delay the onset of clinical signs and mortality post ASFV challenge (21–26). Despite that ASFV-specific antibodies can mediate virus neutralization in plaque reduction assays, a fraction of the infective virus populations remains nonneutralizable even under the circumstance of high antibody titers (21, 26). Moreover, sera from pigs immunized with live-attenuated ASFV and fully protected against parental virus displayed incomplete neutralization with dose-dependent neutralizing efficacies (21, 22, 26). Paradoxes as such suggest the existence of thus far unidentified mechanisms for ASFV dissemination and evasion of humoral immunity.

Extracellular vesicles (EVs) are lipid bilayer-enveloped nanoparticles that are derived from cells and found in plasma, serum, urine, and many other biophysiological fluids (27, 28). EVs are divided into three major subgroups by size, biogenesis, content, and function, including exosomes (40 to 100 nm), microvesicles (100 to 500 nm), and apoptotic bodies (500 to 5,000 nm) (27–29). EV lipid membrane offers protection for their cargo transferring

Author affiliations: [a]National Key Laboratory of Veterinary Public Health Security, Key Laboratory of Animal Epidemiology of the Ministry of Agriculture and Rural Affairs, College of Veterinary Medicine, China Agricultural University, Beijing 100193, People's Republic of China; and [b]China Animal Disease Control Center, Beijing 100125, People's Republic of China

Author contributions: L.Z., J.H., and H.Y. designed research; P.G., J.W., W.W., H.W., M.Y., and Y.Q. performed research; P.G., L.Z., J.W., H.W., Y.H., Y.Z., X. Ge, and X. Guo contributed new reagents/analytic tools; P.G., L.Z., X. Ge, J.H., and H.Y. analyzed data; and P.G., J.H., and H.Y. wrote the paper.

The authors declare no competing interest.

This article is a PNAS Direct Submission.

[1]P.G., L.Z., and J.W. contributed equally to this work.

[2]To whom correspondence may be addressed. Email: hanx0158@cau.edu.cn or yanghanchun1@cau.edu.cn.

This article contains supporting information online at https://www.pnas.org/lookup/suppl/doi:10.1073/pnas.2309506120/-/DCSupplemental.

Published November 20, 2023.

to recipient cells from degradation catalysts and other destructive substances that may exist in extracellular spaces. They carry cellular or viral components as cargo such as nucleic acids, proteins, and virions for intercellular communication (28, 30). Especially, viruses could utilize EVs for cell-to-cell transmission (27, 31–36). This strategy can give many viruses the ability to evade host immune surveillance and antibody neutralization, which is conducive to the efficient viral spread and pathogenesis (31). Since ASFV has been reported to induce cellular apoptosis at late stage of infection (37, 38), we hypothesize that ASFV might utilize EVs for cell-to-cell transmission. We show that the apoptotic bodies (ApoBDs) derived from ASFV-infected macrophages contain viral particles, and ASFV could selectively exploit ApoBD efferocytosis as an alternative pathway for virus entry and cell–cell transmission. The detailed results are described below.

Results

ASFV Induces Apoptosis of Primary Macrophages to Shed ApoBDs. The diameter of ASFV particles is approximately 200 nm (9). If the intercellular transmission of this virus happens, the apoptotic bodies (ApoBDs) will be the most ideal EVs for delivering ASFV particles considering their large sizes. In line with this hypothesis, ASFV encodes a number of proteins for regulating cellular apoptosis, including anti-apoptotic proteins (e.g., A179L, A224L, DP71L, EP153R, etc.) and pro-apoptotic proteins (e.g., p54, E199L, etc.) (38–41). To understand the temporal dynamics of apoptotic induction, we infected primary porcine alveolar macrophages (PAMs) with ASFV strain HN09 at a multiplicity of infection (MOI) of 0.1 and monitored the activation of caspase-3 in a time course manner (Fig. 1). The cleaved form of caspase-3 was detectable around 12 hours post infection (hpi), became visibly increased at 24 hpi, and then reached the plateau around 48 to 60 hpi (Fig. 1*A*), a time point when the virus replication hit the peak (Fig. 1*B*). The same was observed for the infection by a green fluorescent protein (GFP)-tagged recombinant virus (ASFV-GFP), in which the MGF360-18R loci was replaced by GFP under p72 promoter while the substitution did not affect virus growth or interferon induction (*SI Appendix*, Fig. S1 *A–D*). The differential interference contrast (DIC) microscopy revealed in both cases the membrane-blebbing morphology of infected PAMs that gave rise to large EVs, which were similar to the size of ApoBDs (Fig. 1 *C* and *E*; *SI Appendix*, Fig. S1 *E* and *G*). The results were further confirmed by transmission electron microscopy (TEM) showing that the large EVs were around the ASFV-positive PAMs and contained a variety of cellular components (Fig. 1*D* and *SI Appendix*, Fig. S1*F*). DNA staining confirmed that ASFV-infected PAMs underwent nuclear fragmentation and chromatin condensation (*SI Appendix*, Fig. S1*H*).

The identity of the large EVs was further validated by staining of ASFV-GFP-infected PAMs with Alexa-568-conjugated Annexin V (A5-Alexa568), a cell nonpermeable fluorescent reporter for phosphatidylserine (PS) lipids being on the outer leaflet of plasma membrane as a hallmark of apoptotic cells or ApoBDs. Meanwhile, the cells were treated with staurosporine (STS) as a positive control. The entire plasma membrane of ASFV-GFP-infected or STS-treated PAMs as well as the EVs were positive for Annexin V (Fig. 1*F* and *SI Appendix*, Fig. S2 *A* and *B*). Further three-dimensional (3D) reconstruction revealed that the GFP sphere was entirely enclosed by Annexin V-positive membranes (Fig. 1*F* and *SI Appendix*, Fig. S2*C*). Moreover, ASFV-GFP-infected PAMs continuously shed GFP-positive vesicles with increasing amount as the infection progressed as revealed by live-cell imaging (*SI Appendix*, Fig. S3 *A* and *B* and Movie S1). Thus, ASFV infection can actively lead to cell apoptosis and formation of ApoBDs.

ASFV-Containing ApoBDs Can Be Swallowed by Neighboring Macrophages to Establish a Secondary Infection. We performed a more detailed time-course assay to understand the tempodynamics of ApoBD formation by using WT ASFV. The time-lapse confocal/DIC imaging showed that only a few ApoBDs were observed at early stages (6 to 12 hpi) in a high-dose infection (MOI = 10), whereas large numbers of ApoBDs were formed around 18 hpi (*SI Appendix*, Fig. S4 *A* and *B*), fitting well with the documented viral replication cycle (42). At later time point, many cells detached from plates. In a low-dose infection (MOI = 0.1), the ASFV-associated ApoBDs became detectable around 24 hpi and were produced in large amount around 48 to 60 hpi (*SI Appendix*, Fig. S5*A*), coinciding with detectable caspase-3 activation (Fig. 1*A* and *SI Appendix*, Fig. S1*C*). Interestingly, this phenomenon was not observed in PAMs infected with porcine reproductive and respiratory syndrome virus (PRRSV) (*SI Appendix*, Fig. S5*B*), an arterivirus of swine that also induces cellular apoptosis (43). Further analyses by IFA and DIC showed that ASFV infection induced beaded-apoptopodia containing ASFV structural protein p30 and other viral proteins, and these filopodia radiated outward from the center of apoptotic cells to neighboring ASFV-negative macrophages (Fig. 2*A* and *SI Appendix*, Fig. S6 *A–C*). Further TEM analysis demonstrated that the beaded-apoptopodia contained lots of virion particles (Fig. 2 *B*, *Top*) and so were the shedded ApoBDs (Fig. 2 *B*, *Bottom*).

We used ASFV-GFP to infect PAMs at a low MOI to track the release and movement of ApoBDs and to determine whether those GFP-positive ApoBDs could be phagocytosed via neighboring cells to induce a secondary infection. The time-lapse live-cell imaging showed that the infected PAMs undergo membrane-blebbing, induction of ApoBDs, and subsequent transmission of GFP-positive ApoBDs to a recipient cell to establish a productive infection (Fig. 2*C* and Movie S2). Interestingly, once the ApoBD contacted a recipient cell, it could be quickly phagocytosed; this was accompanied by quick disappearance of GFP fluorescence (likely being quenched in an acidic environment and then degraded) and then a slow reappearance of GFP fluorescence around 6 h post phagocytosis (Movie S2), suggesting the start of a new infection. Representative images along the time course in the video are shown in Fig. 2*C*. Thus, ApoBDs can serve as a vehicle for ASFV spread in macrophages.

The Virions Loaded within ApoBDs Are Exclusive Particles Devoid of the Viral Outer Membrane. The TEM showed that there were three forms of ASFV particles in infected cell culture, and these include intracellular virions, extracellular virions, and ApoBD-associated virions (Fig. 3*A*). Both intracellular and ApoBD-associated virions lacked the outer layer membrane and were hence termed as single-membrane viruses. In contrast, the extracellular virions possess the outer layer membrane and were morphologically mature and hence termed double-membrane viruses.

To further characterize the biological property, we isolated ApoBDs along with the other two forms of ASFV from ASFV-infected PAMs according to a previously established differential centrifugation procedure (33, 44) as outlined in Fig. 3*B*. The isolated ApoBDs had a high quality (96%) as monitored by TEM, and it was rare to see the contamination by extracellular virions (Fig. 3*C* and *SI Appendix*, Table S1). In addition, both ApoBDs and extracellular virions were strongly positive for PS as analyzed by dot blot assay. In contrast, the signal was very weak for intracellular virions, which was suspected to be a background binding (Fig. 3*D*). The three fractions were all positive for ASFV nucleic acid as determined by qPCR analysis targeting ASFV *B646L* gene encoding p72 protein (Fig. 3*E*), and they were all infectious in PAMs (Fig. 3*F* and

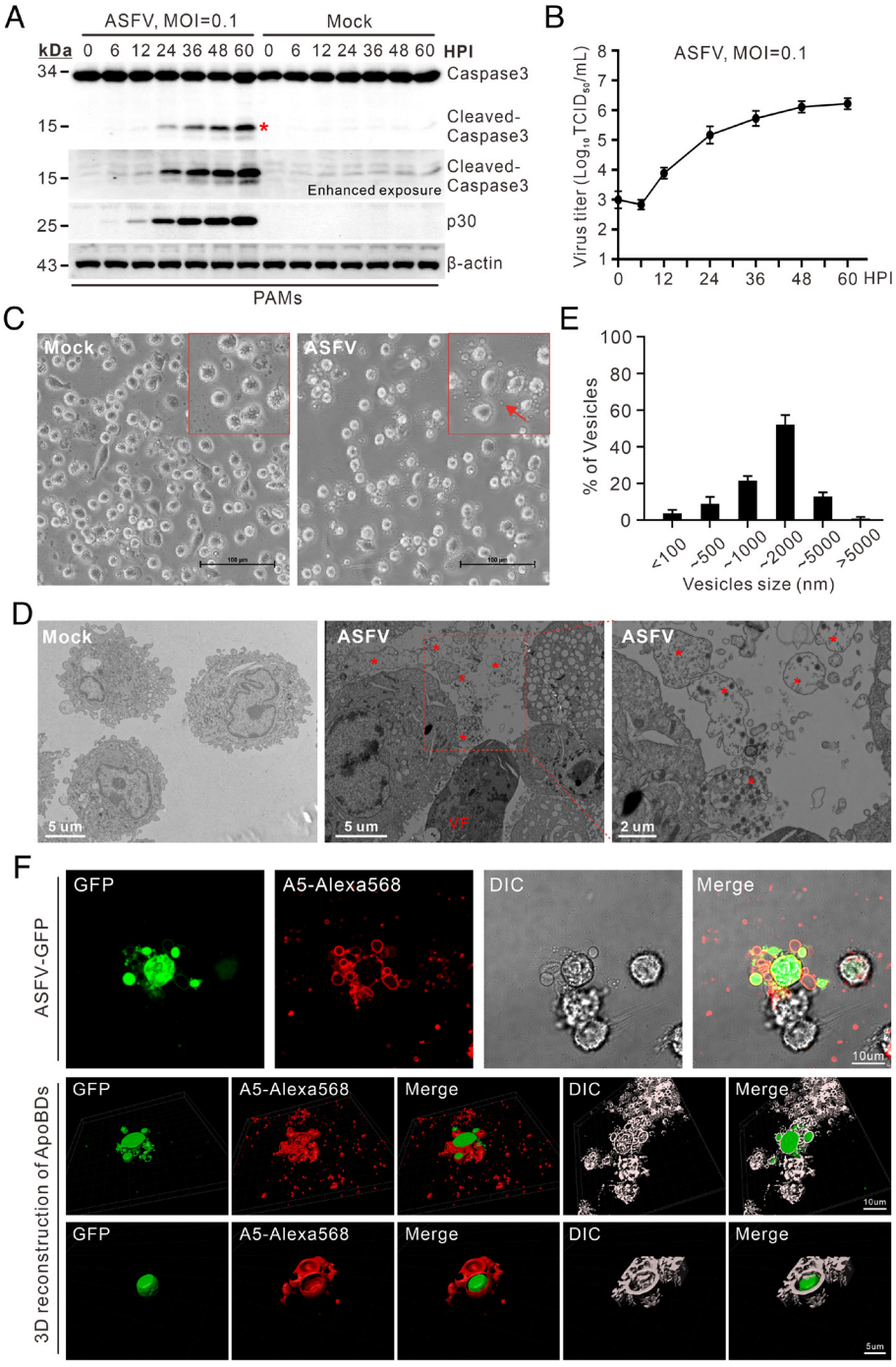

Fig. 1. ASFV induces apoptosis of PAMs to shed ApoBDs. (*A*) Analysis of cellular apoptosis of ASFV-infected cells. PAMs were mock-infected or infected with ASFV strain HN09 at an MOI of 0.1 and harvested at indicated times post infection for Western blot with indicated antibodies to caspase-3, β-actin, and p30. β-actin served as a loading control, and ASFV p30 was used as an indicator of infection. (*B*) Growth kinetics of ASFV HN09 in PAMs at an MOI of 0.1. (*C*) Representative images showing the formation of ApoBDs. PAMs were mock-infected or infected with ASFV strain HN09 at an MOI of 0.1 and analyzed by DIC microscopy at 48 hpi. (*D*) Mock- and ASFV-infected PAMs (MOI = 0.1) were fixed at 48 hpi and analyzed by TEM. The characteristic ApoBDs (asterisk) and viral factory could be visualized only in ASFV-infected cells. (*E*) Size distribution of the vesicles around ASFV-infected PAMs (N = 100). The size of vesicles was measured via the scale bar under light microscope and electron microscope. (*F*) Immunostaining and 3D reconstruction of the ApoBDs. PAMs were infected with ASFV-GFP and stained with A5-Alexa568 at 48 hpi, and the images were reconstructed by Imaris software. Data information: The images were acquired by Nikon A1 confocal microscope and HITACHI HT7700 electron microscope.

SI Appendix, Fig. S7*A*). As a control, the arterivirus PRRSV induced much less shedding of ApoBDs (Fig. 3*F* and *SI Appendix*, Fig. S5*B*). To further distinguish the nature of ApoBDs from extracellular viruses and to rule out the possibility of contamination by extracellular viruses, we performed a precipitation and dilution assay (Fig. 3 *G* and *H*). Series of dilution led to a significant reduction of virus titer in the supernatants (extracellular virions), but did not affect the viruses within the ApoBDs (Fig. 3*H*).

Purified ASFV-Containing ApoBDs Can Be Directly Engulfed by Naive PAMs to Establish a Productive Infection. To further characterize the infection process of ApoBDs, the ApoBDs isolated from ASFV-infected PAMs were incubated with PAMs at 37 °C for 2 h before fixation and staining with monoclonal antibody to p30 or swine serum to ASFV to investigate the vesicle uptake. The confocal microscopy showed that the staining-positive ApoBDs could be engulfed by PAMs (Fig. 4 *A* and *B*). The live-cell imaging showed that GFP-positive ApoBDs were engulfed by PAMs and then gradually lost the fluorescence. At 9 to 12 hpi, the cell began to accumulate visible GFP within gradually increasing fluorescence intensity, suggesting a productive infection (Fig. 4*C* and Movie S3). We also labeled the ApoBDs with A5-Alexa568, showing the signal colocalization of GFP and A5-Alexa568, and the result was the same (*SI Appendix*, Fig. S6*D* and Movie S4). Thus, these results provide strong evidence that ApoBDs can transmit ASFV particles to naive PAMs to establish an infection.

The production kinetics of three forms of virions was subsequently measured by multistep growth curve analysis at an MOI of 0.1 or 0.01. The virions in ApoBDs were kept at a very low level at early stage of infection as compared with the amount of

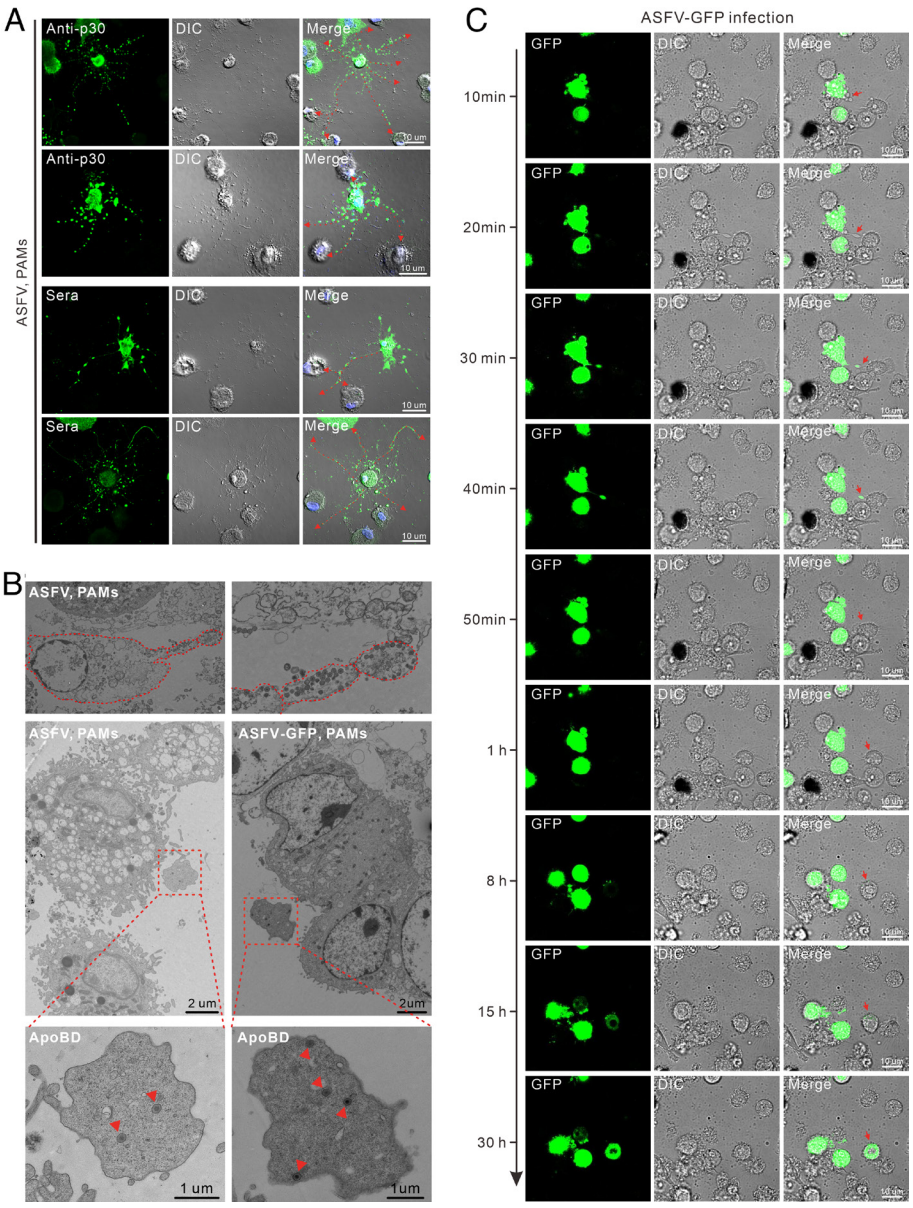

Fig. 2. ApoBDs derived from ASFV-infected PAMs can be swallowed by neighboring PAMs to establish a secondary infection. (*A*) Distribution pattern of the ASFV-positive ApoBDs. PAMs on coverslips in six-well plates were mock or infected with ASFV strain HN09 at an MOI of 0.1. The cells were fixed, permeablized, stained with indicated antibodies, and examined by confocal and DIC microscopy at 48 hpi. The arrows indicated the spreading trend of ASFV-positive ApoBDs. (*B*) ASFV-infected PAMs were fixed at 48 hpi and analyzed by TEM. (*C*) Live-cell imaging of the infection dynamics of ASFV-GFP-infected PAMs and GFP-positive ApoBDs. PAMs were seeded into 35-mm dishes and infected with ASFV-GFP at an MOI of 0.01. At 36 hpi, cells were imaged for time-lapse DIC and confocal microscopy. Representative images were collected from the taken video at the indicated time points. Data information: The images were acquired by Nikon A1 confocal microscope and HITACHI HT7700 electron microscope.

extracellular and intracellular virions, but as the infection progressed, the ApoBD-associated viral titer increased rapidly, coinciding with the induction of apoptosis (Fig. 1*A* and *SI Appendix*, Fig. S1*C*), and reached to a level comparable to the amount of intracellular virions at 36 to 48 hpi (Fig. 4*D*). At the end of infection, the ApoBD-associated virions became a predominant form (Fig. 4*D*).

We also investigated the effect of intervention of cell apoptosis or ApoBD formation on viral propagation. We used two drugs, namely Z-VAD-FMK, a cell-permeable pan-caspase inhibitor, and sertraline (Sert), a well-described antidepressant drug that was identified as an inhibitor of ApoBD formation without affecting apoptosis and membrane blebs (45). Treatment with either Z-VAD-FMK or Sert barely impaired the ASFV replication but specifically suppressed the ApoBD formation (*SI Appendix*, Fig. S7 *B* and *C*). As a result, this resulted in a significant reduction of ApoBD-associated ASFV, but not the total and intracellular virus yield (*SI Appendix*, Fig. S7*C*). Thus, the induction of ApoBDs is not necessary for ASFV replication, but rather serves as a purpose for viral cell–cell transmission.

ApoBD-Mediated Viral Transmission Is Dependent on Both the PS Lipids and Efferocytosis Receptor TIM4. Phosphatidylserine (PS) is a classical "eat-me" signal that normally resides in the inner leaflet of the plasma membrane but flips to the outer membrane of dying cells and ApoBDs (46). This signal can be recognized via phagocyte receptors, i.e., Gas6, MFG-E8, TIM4, etc., and masked via PS-binding protein Annexin V (46, 47). We prepared intracellular virions, extracellular virions, and ASFV-containing ApoBDs and incubated them, respectively, with Annexin V protein prior to exposure to naive PAMs. Strikingly, treatment with Annexin V significantly inhibited ApoBD-mediated ASFV infection in a dose-dependent manner (Fig. 5 *A*–*D*). It also exhibited an inhibitory effect on extracellular virions, which is not surprising as they also were positive for PS in the out leaflet (Fig. 3*D*). As expected, the treatment did not have effect on the infection of intracellular virions at all (Fig. 5 *A* and *B*). Thus, the PS is an important factor mediating the infection of both extracellular and ApoBD-associated ASFV infection.

We next determined whether the ApoBD-associated ASFV required the efferocytosis receptors on the PAMs for infection.

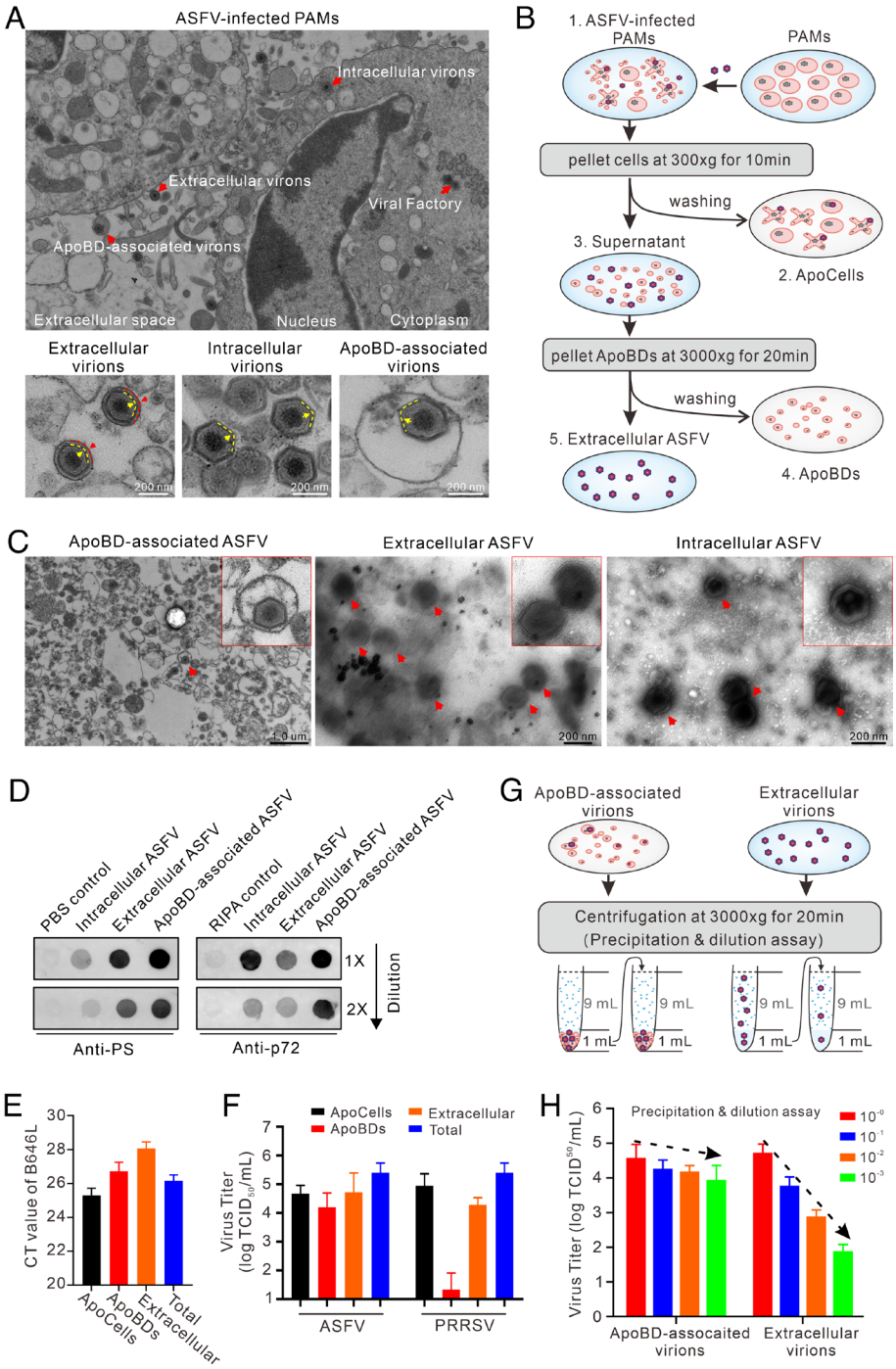

Fig. 3. Purified ApoBDs from ASFV-infected PAMs contain infectious virions. (*A*) Presence of different forms of virions in ASFV-infected PAMs. (*B*) Schematic diagram of the procedure for purifying ApoBDs via differential centrifugation. PAMs seeded T-25 flask were infected with ASFV strain HN09 at an MOI of 0.1. At 60 hpi, the cells and culture were harvested for isolation of ApoBDs. (*C*) TEM analysis of the isolated ApoBDs, extracellular virions, and intracellular virions from ASFV-infected PAMs. (*D*) Dot blot analysis of PS of the three forms of virions. The purified virions were resuspended in phosphate buffered saline (PBS) (not to destroy the membrane) or lysed in Radio-Immunoprecipitation Assay (RIPA) buffer, and then spotted onto nitrocellulose membranes, followed by detection with indicated antibodies. PBS or RIPA was spotted as a negative control. (*E*) qPCR analysis of ASFV nucleic acid in different fractions. (*F*) Titration of ASFV and PRRSV load of different fractions in PAMs by $TCID_{50}$. (*G*) Schematic presentation of the precipitation and dilution assay. The ApoBD-associated and extracellular virions were isolated same as (*B*) and centrifuged at 3,000 g for 20 min to collect the supernatant, and the pellet was then resuspended by RPMI-1640. (*H*) $TCID_{50}$ analysis of virus titer after dilution. Data information: The images were acquired by HITACHI HT7700 electron microscope.

We tested several antibodies against efferocytosis receptors such as Gas6, MFG-E8, and TIM4 but unfortunately only the anti-TIM4 antibody reacted well with PAMs. We found that pretreatment of PAMs with antibodies to TIM4 significantly inhibited ApoBD-mediated ASFV infectivity, and this operated in a dose-dependent manner (Fig. 6 *A*–*C*) and that the infectivity of the extracellular virions could also be inhibited to some extent about 40 to 50% (Fig. 6 *A* and *B*). In contrast, the infectivity of the intracellular ASFV was not affected as expected (Fig. 6 *A* and *B*). Meanwhile, overexpression of TIM4 or MFG-E8 significantly increased the viral production in extracellular and ApoBD-associated ASFV-infected wild boar lung (WSL) cells by about half a log (Fig. 6 *D* and *E*), suggesting that TIM4 and MFG-E8 are critical factors for ASFV entry into cells. Together, the above results

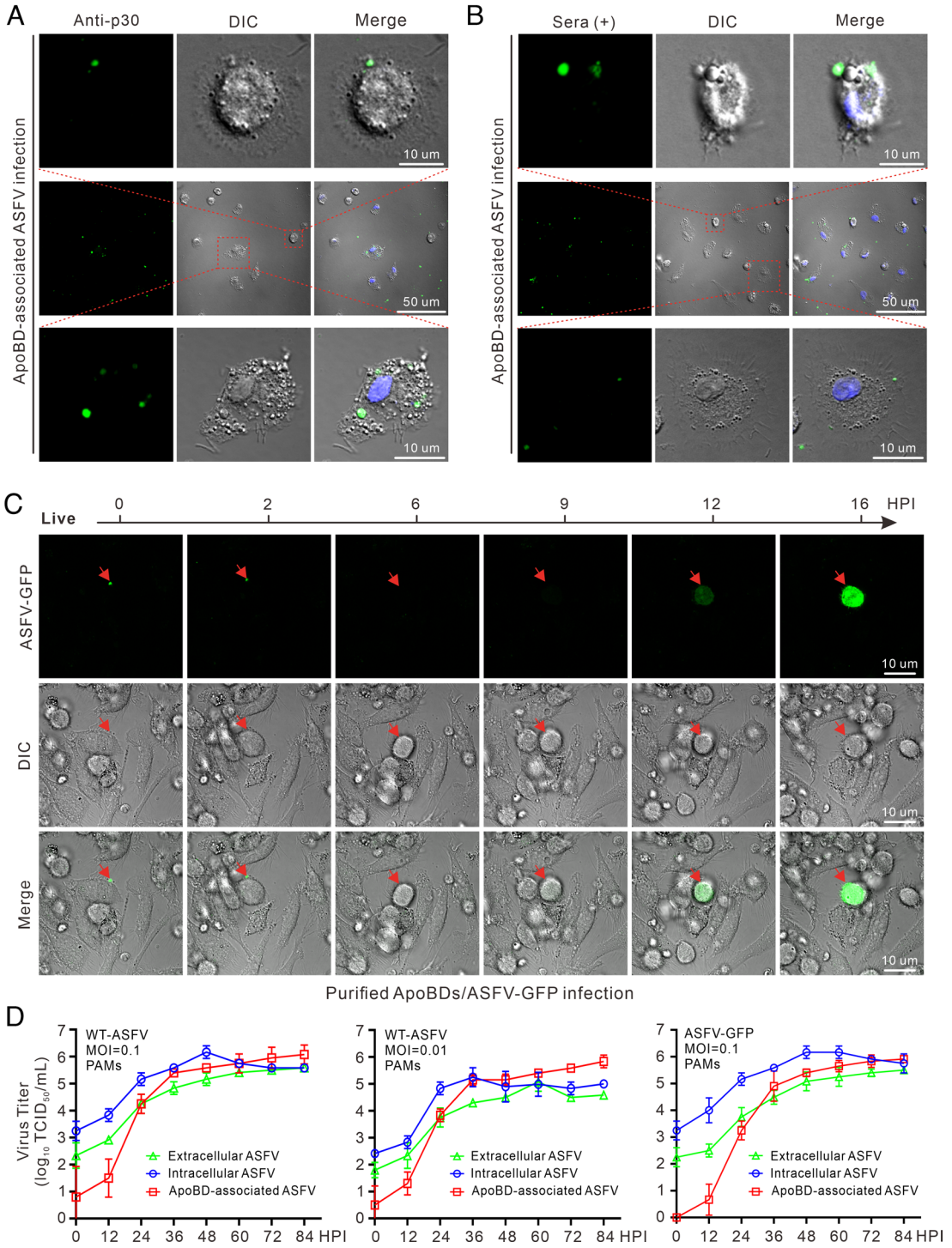

Fig. 4. The purified ASFV-containing ApoBDs can transmit ASFV and establish a productive infection. PAMs grown on coverslips in six-well plates were incubated with the purified ApoBDs from WT ASFV-infected PAMs at 37 °C for 2 h, followed by cell fixation, permeablization, and staining with the antibodies to p30 (*A*) or swine serum to ASFV (*B*). (*C*) Live-cell imaging of the infection dynamics of the ApoBDs purified from ASFV-GFP-infected PAMs. Representative images were collected from the taken video at indicated time points. Data information: The images were acquired by Nikon A1 confocal microscope. (*D*) The dynamics of viral load in different fractions. PAMs were infected with WT ASFV or ASFV-GFP at an MOI of 0.1 or 0.01. At indicated time points, the three forms of virions were isolated and titrated by $TCID_{50}$ in PAMs.

suggest that the ASFV-containing ApoBDs can utilize the conventional apoptotic uptake pathway to cell-to-cell transmission.

ApoBD-Mediated Viral Transmission Is Fully Resistant to Swine Sera to ASFV. We investigated ApoBD-mediated ASFV transmission in the presence of swine serum to ASFV. The serum had an IFA titer of more than 50,000 (Fig. 7*A*) and could inhibit the infection efficiency of intracellular virions by about 64% and reduced the virion production by about 0.5 log but displayed no effect on extracellular and ApoBD-associated virions (Fig. 7 *B*–*D*). However, when the membrane integrity of the ApoBDs was disrupted by three cycles of quick freeze–thaw, the released single-membrane virions became susceptible to serum neutralization, and the anti-ASFV serum could inhibit the infectivity by about 53%

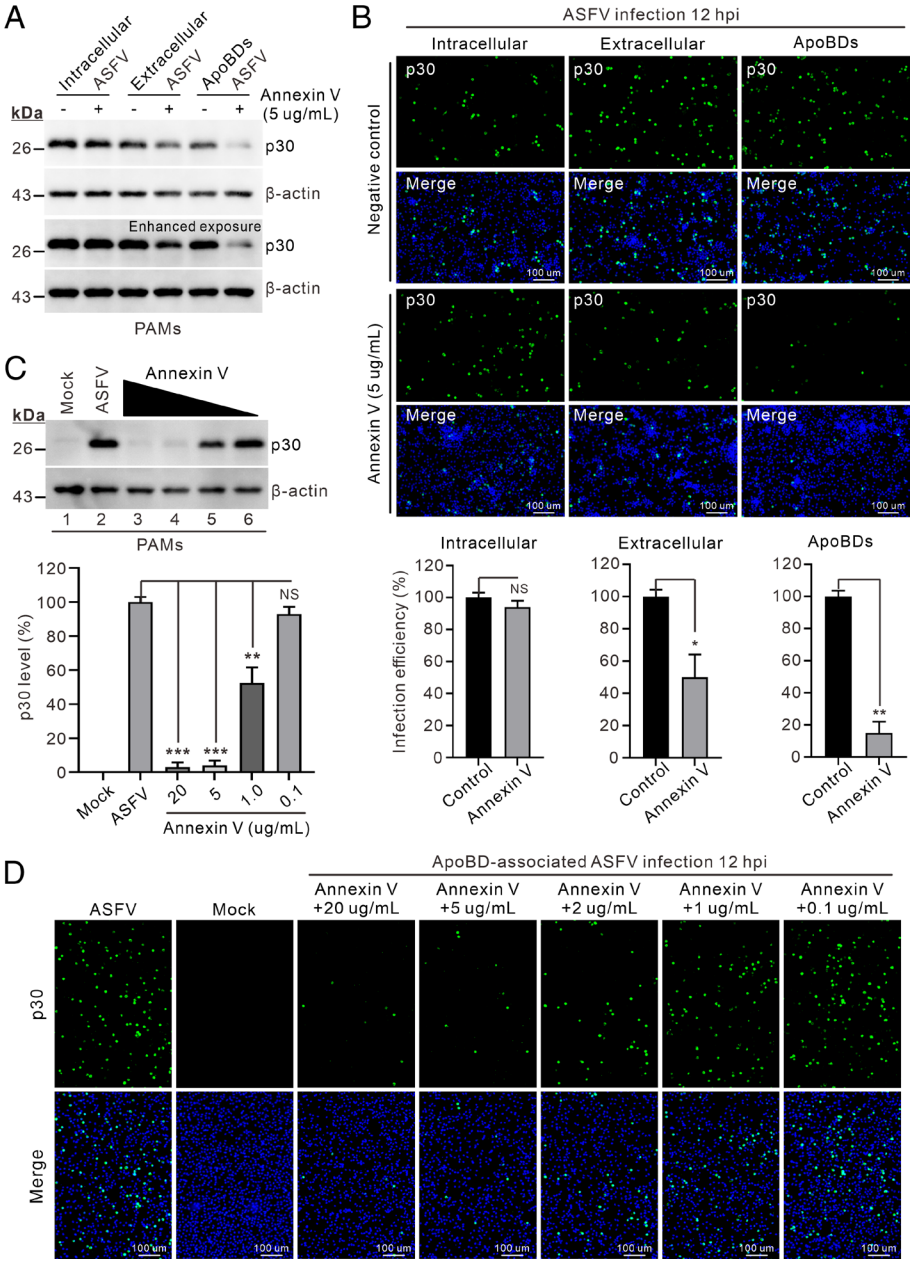

Fig. 5. Blocking PS lipids suppresses ApoBD-mediated ASFV infection. Different forms of ASFV were isolated at 48 hpi from PAMs infected with ASFV strain HN09 at an MOI of 0.1 and then incubated, respectively, with Annexin V protein (5 μg/mL) prior to exposure to naive PAMs seeded in 24-well plates. The effect on viral replication was determined by Western blot (*A*) and IFA analysis (*B*). The infection efficiency was expressed as proportion of p30-positive cells via comparing Annexin V-treated group with control group, respectively. (*C*) Dose-dependent effect of Annexin V on ASFV infection by Western blot analysis. The relative band density of p30 was expressed as percentage compared to the untreated ASFV control (lane 2) after being normalized against β-actin in the corresponding lane. (*D*) Dose-dependent effect of Annexin V on the infection of ApoBD-associated virions by IFA analysis. Data information: Error bars indicate means ± SDs.

(*SI Appendix*, Fig. S8*A*). As expected, the virions released from ApoBDs were not susceptible to the treatment of either Annexin V or anti-TIM4 antibody (*SI Appendix*, Fig. S8 *B* and *C*). Thus, the ApoBD-mediated antibody evasion depends on its membrane integrity, and the findings highlight efferocytosis as a critical means for ASFV evasion of antibody neutralization.

Discussion

Clinical infections by ASFV often cause hemorrhagic fever of pigs with high fatality and can also lead to persistent infections in the presence of antibodies for years (21, 22, 48). Prominently, immune swine sera are not capable of mediating a complete neutralization of ASFV in vitro (21, 22), and the mechanisms involved have remained not fully understood. In this study, we report that ASFV takes advantage of the cellular apoptotic pathway and rides the ApoBDs as a form of delivering vehicles for cell–cell transmission. These vesicles contain infectious but outer layer membrane-free viral particles and are resistant to treatment of neutralizing antibodies. In addition, we identified PS and TIM4 as critical host factors for mediating virus transmission. A model for ASFV cell-to-cell transmission is proposed in Fig. 8.

Extracellular vesicles play a critical role in intercellular communications by transporting intracellular biomolecules (nucleic acids, proteins, and lipids) (28, 30). Increasing evidence has indicated that many viruses use this mechanism for spread in vivo (27, 31).

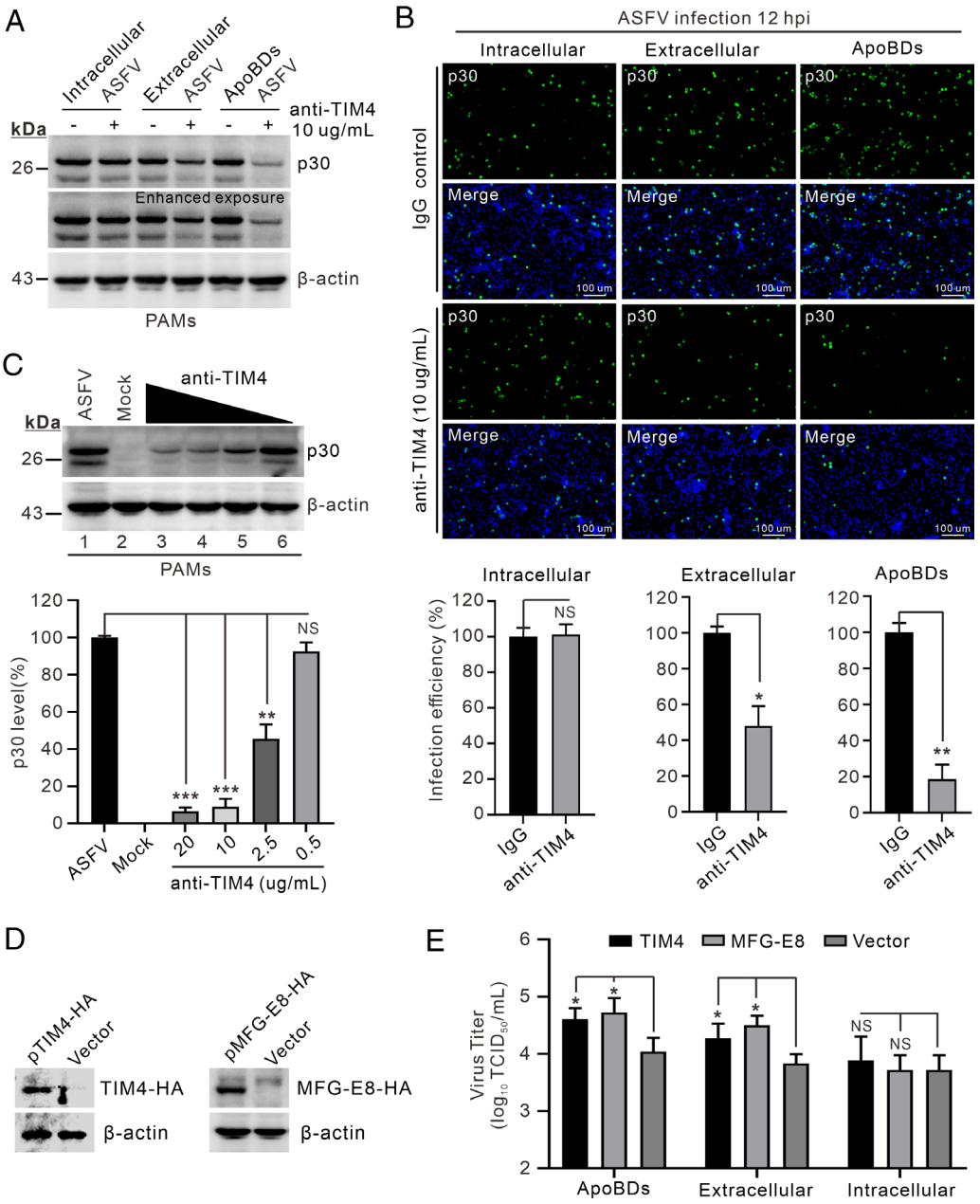

Fig. 6. ApoBD-mediated ASFV infection is dependent on the efferocytosis receptor TIM4. (*A*) PAMs in 24-well plates were incubated with antibodies to TIM4 (10 μg/mL) or isotype IgG for 1 h and then exposed to three forms of virions before performing Western blot analysis at 12 hpi. (*B*) The same as (*A*), except by IFA analysis. The infection efficiency was expressed as proportion of p30-positive cells via comparing anti-TIM4 antibody treated group with that of isotype IgG-treated group, respectively. (*C*) Dose-dependent analysis. The same as (*A*) except that different doses of anti-TIM4 antibody was used. The relative band density of p30 was expressed as percentage compared to the ASFV infection control (lane 1) after being normalized against β-actin in the corresponding lane. (*D* and *E*) Effect of overexpression of TIM4 or MFG-E8 on the replication of ASFV in WSL-R4 cells. WSL-R4 cells in 12-well plates were transfected with pCMV-TIM4-HA, pCMV-MFG-E8-HA, or vector control (1.5 μg). At 24 h posttransfection, the cells were subjected to Western blot analysis with antibodies to HA tag (*D*) or infected with three forms of virions at an MOI of 1.0 for 24 h before being harvested for titration (*E*). Data information: Error bars indicate means ± SDs.

Currently, most studies have focused on the utilization of exosomes as an efficient cell-to-cell transmission system, and this is exemplified by many small-to-medium size viruses, even including those nonenveloped viruses, such as hepatitis A virus (HAV), severe acute respiratory syndrome coronavirus 2 (SARS-CoV-2), HIV, Hepatitis C virus (HCV), herpesviruses, polyomavirus, rotaviruses, noroviruses, and so on (27, 31–33, 35, 36, 49–51). However, host cells also shed other types of vesicles, including macrovesicles and ApoBDs (28, 31). For the latter, ApoBDs are large vesicles that originate from apoptotic cells and contain residual ingredients of dying cells with a diameter of 500 to 5,000 nm (46). These vesicles are normally phagocytosed by macrophages to prevent deleterious impact on the surroundings (46, 47). Although it is common that many viruses use apoptotic mimicry to enhance virus entry and spread (33, 34, 52–54), this mechanism in most reported cases is carried out in the form of progeny virions by packing PS into viral envelope when viruses bud through the cell plasma membrane (e.g., Ebola virus, vaccinia virus, flaviviruses, arena viruses, etc.) (34, 55–57). On the other hand, the reports regarding ApoBDs as a form of viral transmission vehicles are scarce. One recent study documented that avian influenza virus (AIV) can utilize the monocyte apoptotic bodies as vehicles for viral propagation (58), but it lacks intuitive evidence, such as using live-cell imaging, to prove AIV transmission via ApoBDs. In this study, we provide strong

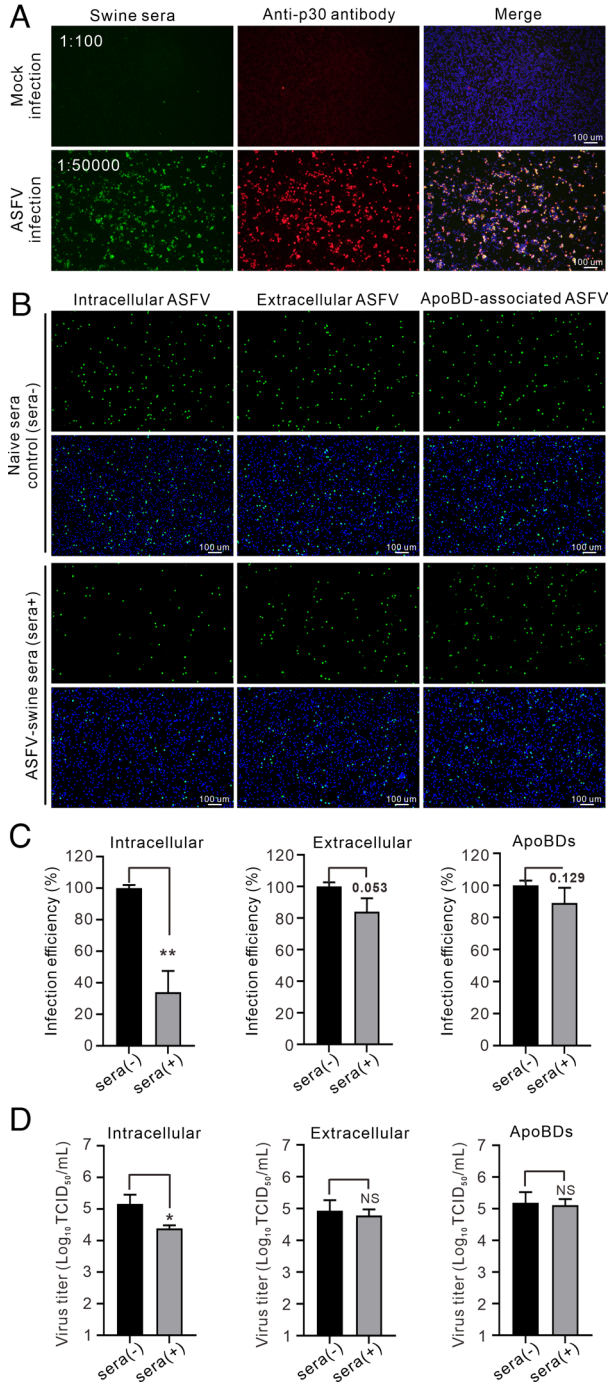

Fig. 7. ApoBD-mediated viral transmission is fully resistant to swine sera to ASFV. (*A*) IFA analysis of the titer of swine anti-ASFV serum in PAMs with the antibody to p30 as a control. (*B–D*) Intracellular virions, extracellular virions, and ASFV-containing ApoBDs were incubated with negative swine serum (−) or ASFV antibody positive swine serum (+) at a volume ratio of 1:1 at 37 °C for 1 h. The mixtures were then incubated with naive PAMs at 37 °C for 1 h followed by washes and addition of culture medium. (*B*) At 12 hpi, the cells were fixed and stained with antibodies to p30 for IFA. (*C*) The infection efficiency of three virion forms was expressed as proportion of p30-positive cells by comparing sera (+) group with sera (−) group, respectively. (*D*) The same as above, but the cells were harvested at 24 hpi for viral titration by $TCID_{50}$. Data information: Error bars indicate means ± SDs.

evidence to show that that ASFV makes use of ApoBDs for virus spread between macrophages (Figs. 2–4).

The establishment of ApoBDs as an efficient transmission route is supported by three lines of evidence. The confocal time-elapse cell imaging provides the real-time, direct evidence to show the dynamic process of apoptotic induction and cell-to-cell transmission by using a GFP-tagged virus as a model organism (Movie S2). The second line of evidence comes from characterization of the in vitro purified ApoBDs. Its identity and purity were confirmed by A5-Alexa568 staining, TEM, IFA, and dot blotting (Figs. 1*F*, 2*B*, and 3 *C–F*). Moreover, a modified dilution assay was used to further distinguish ApoBD-containing virions from the extracellular viruses (Fig. 3 *G* and *H*). The dilutions led to a decrease titer of extracellular free viruses but not the infectivity of virions within ApoBDs (Fig. 3 *G* and *H*). The transmission was further verified by live-cell imaging (Movies S2–S4). The third piece of evidence comes from pharmacological and genetics approaches. Treatment with either Annexin V or anti-TIM4 antibody significantly suppressed the ApoBD-mediated ASFV infection, but not on the infections by virions devoid of the outer membrane (Figs. 5 and 6 *A–C* and *SI Appendix*, Fig. S8 *B* and *C*). Likewise, the swine sera to ASFV exerted no effect on the ApoBD-mediated transmission, but could partially act on the single-membrane virions (Fig. 7 and *SI Appendix*, Fig. S8*A*). These findings suggest that the entry mechanism of single-membrane virions is quite different from ApoBD-associated and the extracellular viruses (double membrane).

The finding of ApoBD-mediated virus spread provides further insight into the ASFV tropism to macrophages. It has been reported that ASFV prefers to infect the monocyte-derived macrophages at an intermediate to late stage of differentiation and that macrophages are about five times more susceptible to ASFV infection than monocytes (21, 22, 59). The high expression level of certain surface markers (e.g., PS, etc.) renders macrophages a higher capacity of phagocytosing apoptotic cells for clearance (22, 60, 61). The utilization of PS-positive ApoBDs for ASFV infection and cell–cell transmission is in line with these reports and explains well at least in part why ASFV prefers macrophages as a primary tropism. In accordance with the tempo-dynamics of virus-induced apoptosis (Fig. 1*A* and *SI Appendix*, Fig. S1*C*), the ApoBDs were induced at late stage of ASFV infection (*SI Appendix*, Fig. S4 and Fig. 5*A*), and the associated viral titer reached to a level comparable to the amount of intracellular virions (Fig. 4*D*). Thus, this process is tailored in a manner ready for the easy phagocytic uptake by macrophages for further cell–cell transmission of progeny virions. As for receptor usages, several receptor candidates, i.e., CD163, CD45, MHC-I, etc., have been proposed as entry receptors (15, 22, 57), but no certain receptor for ASFV entry has yet been indispensable, indicating the complexity of ASFV entry and transmission. As compared to the receptor-mediated endocytosis, the ApoBD-mediated spread of ASFV represents a rather less restricted, complementary entry mechanism conducive to virus spread in the presence of selective immune pressures.

We also found that ASFV exists in three forms during infection (Fig. 3*A*) and that both extracellular and ApoBD-containing virions, but not the single-membrane virions, were resistant to antibody neutralization (Fig. 7 and *SI Appendix*, Fig. S8*A*). Thus, the hijack of the cellular apoptotic uptake pathway provides an efficient means of immune evasion (e.g., inflammation induction, antibody neutralization, etc.) and a quick and economical way of virus spread (no need of outer membrane). The findings provide an explanation on why the sera from animals infected with ASFV often lack neutralizing activity and thus have important implications in ASFV control and vaccine development. In addition, the results provide insight into transmission of large DNA viruses, especially giant viruses.

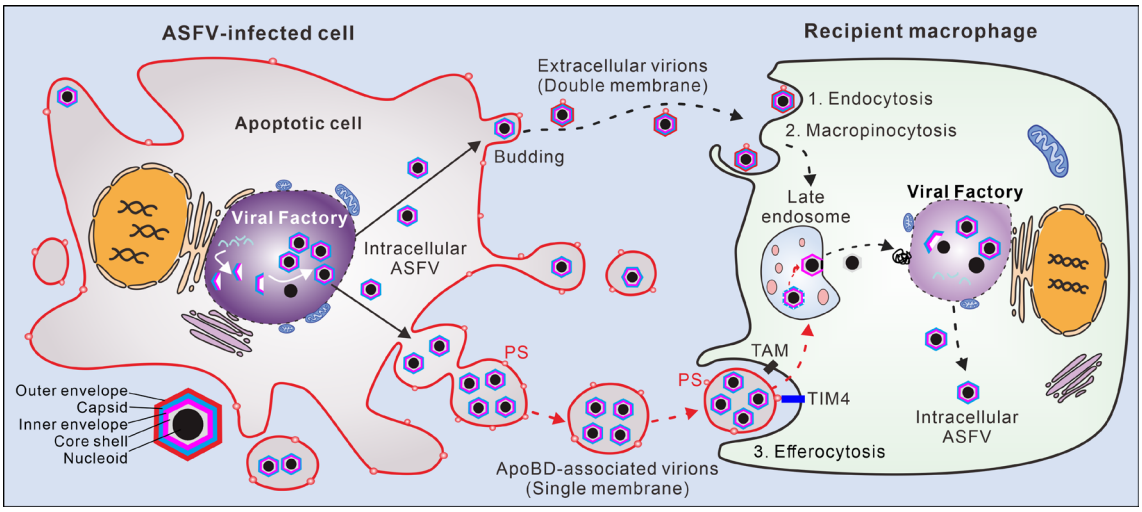

Fig. 8. A proposed model for ASFV transmission. ASFV induces cell apoptosis to shed the virion-loaded ApoBDs at late stage of infection via caspase-3 activation. The PS-positive ApoBDs carrying single-membrane virions are then phagocytosed by neighboring PAMs via PS interaction with efferocytosis receptors (e.g., TIM4, MFG-E8, etc.). Meanwhile, ASFV particles can directly bud from plasma membrane to acquire the PS-positive outer membrane. These extracellular virions can enter into recipient PAMs by means of either efferocytosis, clathrin-mediated endocytosis, or macropinocytosis.

Materials and Methods

Reagents. Primary PAMs from 1-mo-old SPF piglets and WSL cells were maintained in RPMI-1640 medium. Type II ASFV strain CADC_HN09 (GenBank accession no: MZ614662.1) was used a model organism in this study. The commercial antibodies and chemicals are from various sources, and the plasmids were engineered by standard recombinant DNA procedures.

ApoBD Isolation. ApoBDs were purified from ASFV-infected PAMs via differential centrifugation. Briefly, the samples were centrifuged at 300 g to obtain the ApoCells-enriched fraction, whereas the supernatant containing ApoBDs was centrifuged at 3,000 g to pellet ApoBDs. Purified-ApoBD samples were validated by DIC microscopy and transmission electron microscopy.

Blocking Assay. The isolated ApoBDs were incubated with Annexin V or swine sera for 1 h prior to infection of recipient PAMs. To block the function of efferocytosis receptor on recipient PAMs, the cells were incubated with anti-TIM4 antibody prior to incubation with ApoBDs. The unbound viruses or ApoBDs were washed off with serum-free RPMI-1640, and the cells were cultured in maintenance medium containing 2% FBS. ASFV replication was measured at 12 or 24 hpi by western analysis and IFA.

Annexin V Conjugates for Apoptosis Detection. PAMs were washed with annexin-binding buffer and incubated with the Alexa Fluor® 568 conjugated Annexin V for 15 min before being washed three times and observed with a fluorescence microscope.

Construction of Recombinant ASFV. The GFP was inserted to replace the loci MGF360-18R under the control of p72 promoter. The recombinant virus ASFV-GFP was generated via homologous recombination, followed by successive rounds of plaque assay in PAMs, and confirmed by PCR.

Live-Cell Imaging. PAMs on coverslip-bottomed dishes were infected with ASFV-GFP or purified ApoBDs and imaged for time-lapse and DIC microscopy with a Nikon A1 confocal microscope.

Transmission Electron Microscopy. PAMs or isolated ApoBDs were fixed with 0.1 M phosphate buffer containing 4% paraformaldehyde and 2% glutaraldehyde. The pellet was then enrobed in low melting point agarose and post-fixed in 1% osmium tetroxide in cacodylate buffer and en bloc stained with 1% uranyl acetate. Following dehydration with acetone, it was embedded in epoxy (TAAB 812 resin). After polymerization, 80-nm-thick (ultrathin) sections were obtained and stained with uranyl acetate and lead citrate. Imaging was performed in a HITACHI HT7700 electron microscope.

Statistical Analysis. Statistical significance was analyzed by two-tailed unpaired Student's *t* test. Significance symbols are defined as follows: NS, no significance; $*P < 0.05$; $**P < 0.01$; $***P < 0.001$. Error bars indicate means ± SD. Detailed descriptions are provided in *SI Appendix, Materials and Methods*.

Data, Materials, and Software Availability. All study data are included in the article and/or supporting information.

ACKNOWLEDGMENTS. This study was supported by the National Key Research and Development Program of China (2021YFD1800100), the National Natural Science foundation of China (32025035), and China Agriculture Research System of Ministry of Finance and Ministry of Agriculture and Rural Affairs (CARS-35).

1. C. L. Netherton, S. Connell, C. T. O. Benfield, L. K. Dixon, The genetics of life and death: Virus-host interactions underpinning resistance to African swine fever, a viral hemorrhagic disease. *Front. Genet.* **10**, 402 (2019).
2. X. Zhou *et al.*, Emergence of African swine fever in China, 2018. *Transbound. Emerg. Dis.* **65**, 1482–1484 (2018).
3. D. Zhao *et al.*, Replication and virulence in pigs of the first African swine fever virus isolated in China. *Emerg. Microbes Infect.* **8**, 438–447 (2019).
4. X. X. Wen *et al.*, Genome sequences derived from pig and dried blood pig feed samples provide important insights into the transmission of African swine fever virus in China in 2018. *Emerg. Microbes Infect.* **8**, 303–306 (2019).
5. E. Mighell, M. P. Ward, African Swine fever spread across Asia, 2018–2019. *Transbound. Emerg. Dis.* **68**, 2722–2732 (2021).
6. K. Stahl *et al.*, Epidemiological analysis of African swine fever in the European Union during 2022. *EFSA J.* **21**, e08016 (2023).
7. M. Arias, C. Jurado, C. Gallardo, J. Fernandez-Pinero, J. M. Sanchez-Vizcaino, Gaps in African swine fever: Analysis and priorities. *Transbound. Emerg. Dis.* **65**, 235–247 (2018).
8. L. M. Iyer, L. Aravind, E. V. Koonin, Common origin of four diverse families of large eukaryotic DNA viruses. *J. Virol.* **75**, 11720–11734 (2001).
9. N. Wang *et al.*, Architecture of African swine fever virus and implications for viral assembly. *Science* **366**, 640–644 (2019).
10. S. Liu *et al.*, Cryo-EM structure of the African swine fever virus. *Cell Host Microbe* **26**, 836–843.e833 (2019).
11. H. Zhang *et al.*, Vaccines for African swine fever: An update. *Front. Microbiol.* **14**, 1139494 (2023).
12. N. N. Gaudreault, D. W. Madden, W. C. Wilson, J. D. Trujillo, J. A. Richt, African swine fever virus: An emerging DNA arbovirus. *Front. Vet. Sci.* **7**, 215 (2020).
13. G. Andres, African swine fever virus gets undressed: New insights on the entry pathway. *J. Virol.* **91**, e01906–e01916 (2017).
14. B. Hernaez, C. Alonso, Dynamin- and clathrin-dependent endocytosis in African swine fever virus entry. *J. Virol.* **84**, 2100–2109 (2010).
15. C. Sanchez-Torres *et al.*, Expression of porcine CD163 on monocytes/macrophages correlates with permissiveness to African swine fever infection. *Arch. Virol.* **148**, 2307–2323 (2003).
16. E. G. Sanchez *et al.*, African swine fever virus uses macropinocytosis to enter host cells. *PLoS Pathogens* **8**, e1002754 (2012).
17. T. Matamoros *et al.*, African swine fever virus protein pE199L mediates virus entry by enabling membrane fusion and core penetration. *mBio* **11**, e00789–e00820 (2020).
18. D. P. Gladue *et al.*, African swine fever virus Gene B117L encodes a small protein endowed with low-ph-dependent membrane permeabilizing activity. *J. Virol.* **97**, e0035023 (2023).

19. I. Rodriguez, M. L. Nogal, M. Redrejo-Rodriguez, M. J. Bustos, M. L. Salas, The African swine fever virus virion membrane protein pE248R is required for virus infectivity and an early postentry event. *J. Virol.* **83**, 12290–12300 (2009).
20. B. Hernaez, M. Guerra, M. L. Salas, G. Andres, African swine fever virus undergoes outer envelope disruption, capsid disassembly and inner envelope fusion before core release from multivesicular endosomes. *PLoS Pathog.* **12**, e1005595 (2016).
21. J. A. Canter *et al.*, Serum neutralizing and enhancing effects on African swine fever virus infectivity in adherent pig PBMC. *Viruses* **14**, 1249 (2022).
22. J. J. Zhu, African swine fever vaccinology: The biological challenges from immunological perspectives. *Viruses* **14**, 2021 (2022).
23. L. Zsak, D. V. Onisk, C. L. Afonso, D. L. Rock, Virulent African swine fever virus isolates are neutralized by swine immune serum and by monoclonal antibodies recognizing a 72-kDa viral protein. *Virology* **196**, 596–602 (1993).
24. P. GomezPuertas *et al.*, Neutralizing antibodies to different proteins of African swine fever virus inhibit both virus attachment and internalization. *J. Virol.* **70**, 5689–5694 (1996).
25. F. Ruiz Gonzalvo, C. Caballero, J. Martinez, M. E. Carnero, Neutralization of African swine fever virus by sera from African swine fever-resistant pigs. *Am. J. Vet. Res.* **47**, 1858–1862 (1986).
26. J. M. Escribano, I. Galindo, C. Alonso, Antibody-mediated neutralization of African swine fever virus: Myths and facts. *Virus Res.* **173**, 101–109 (2013).
27. E. Nolte-'t Hoen, T. Cremer, R. C. Gallo, L. B. Margolis, Extracellular vesicles and viruses: Are they close relatives? *Proc. Natl. Acad. Sci. U.S.A.* **113**, 9155–9161 (2016).
28. M. Tkach, C. Thery, Communication by extracellular vesicles: Where we are and where we need to go. *Cell* **164**, 1226–1232 (2016).
29. R. Kalluri, V. S. LeBleu, The biology, function, and biomedical applications of exosomes. *Science* **367**, eaau6977 (2020).
30. M. Mathieu, L. Martin-Jaular, G. Lavieu, C. Thery, Specificities of secretion and uptake of exosomes and other extracellular vesicles for cell-to-cell communication. *Nat. Cell Biol.* **21**, 9–17 (2019).
31. L. Urbanelli *et al.*, The role of extracellular vesicles in viral infection and transmission. *Vaccines (Basel)* **7**, 102 (2019).
32. C. Zeng *et al.*, SARS-CoV-2 spreads through cell-to-cell transmission. *Proc. Natl. Acad. Sci. U.S.A.* **119**, e2111400119 (2022).
33. Y. H. Chen *et al.*, Phosphatidylserine vesicles enable efficient en bloc transmission of enteroviruses. *Cell* **160**, 619–630 (2015).
34. J. Mercer, A. Helenius, Vaccinia virus uses macropinocytosis and apoptotic mimicry to enter host cells. *Science* **320**, 531–535 (2008).
35. J. Morris-Love *et al.*, JC polyomavirus uses extracellular vesicles to infect target cells. *mBio* **10**, e00379–e00419 (2019).
36. V. Ramakrishnaiah *et al.*, Exosome-mediated transmission of hepatitis C virus between human hepatoma Huh7.5 cells. *Proc. Natl. Acad. Sci. U.S.A.* **110**, 13109–13113 (2013).
37. I. Galindo *et al.*, The ATF6 branch of unfolded protein response and apoptosis are activated to promote African swine fever virus infection. *Cell Death Dis.* **3**, e341 (2012).
38. L. K. Dixon, P. J. Sanchez-Cordon, I. Galindo, C. Alonso, Investigations of pro- and anti-apoptotic factors affecting african swine fever virus replication and pathogenesis. *Viruses* **9**, 241 (2017).
39. T. Li *et al.*, African swine fever virus pE199L induces mitochondrial-dependent apoptosis. *Viruses* **13**, 2240 (2021).
40. F. Zhang, A. Moon, K. Childs, S. Goodbourn, L. K. Dixon, The African swine fever virus DP71L protein recruits the protein phosphatase 1 catalytic subunit to dephosphorylate eIF2alpha and inhibits CHOP induction but is dispensable for these activities during virus infection. *J. Virol.* **84**, 10681–10689 (2010).
41. J. Shi, W. Liu, M. Zhang, J. Sun, X. L. Xu, The A179L gene of African swine fever virus suppresses virus-induced apoptosis but enhances necroptosis. *Viruses* **13**, 2490 (2021).
42. R. Munoz-Moreno, I. Galindo, M. A. Cuesta-Geijo, L. Barrado-Gil, C. Alonso, Host cell targets for African swine fever virus. *Virus Res.* **209**, 118–127 (2015).
43. S. Z. Yuan *et al.*, Induction of apoptosis by the nonstructural protein 4 and 10 of porcine reproductive and respiratory syndrome virus. *Plos One* **11**, e0156518 (2016).
44. T. K. Phan, I. K. Poon, G. K. Atkin-Smith, Detection and isolation of apoptotic bodies to high purity. *J. Vis. Exp.* **12**, 58317 (2018).
45. G. K. Atkin-Smith *et al.*, A novel mechanism of generating extracellular vesicles during apoptosis via a beads-on-a-string membrane structure. *Nat. Commun.* **6**, 7439 (2015).
46. S. Nagata, Apoptosis and clearance of apoptotic cells. *Annu. Rev. Immunol.* **36**, 489–517 (2018).
47. P. Mehrotra, K. S. Ravichandran, Drugging the efferocytosis process: Concepts and opportunities. *Nat. Rev. Drug. Discov.* **21**, 601–620 (2022).
48. L. K. Dixon, H. Sun, H. Roberts, African swine fever. *Antiviral Res.* **165**, 34–41 (2019).
49. L. Martin-Jaular *et al.*, Unbiased proteomic profiling of host cell extracellular vesicle composition and dynamics upon HIV-1 infection. *EMBO J.* **40**, e105492 (2021).
50. J. Dufloo, T. Bruel, O. Schwartz, HIV-1 cell-to-cell transmission and broadly neutralizing antibodies. *Retrovirology* **15**, 51 (2018).
51. M. Santiana *et al.*, Vesicle-cloaked virus clusters are optimal units for inter-organismal viral transmission. *Cell Host Microbe* **24**, 208–220.e208 (2018).
52. X. Wei *et al.*, Porcine reproductive and respiratory syndrome virus utilizes viral apoptotic mimicry as an alternative pathway to infect host cells. *J. Virol.* **94**, e00709–e00720 (2020).
53. A. Amara, J. Mercer, Viral apoptotic mimicry. *Nat. Rev. Microbiol.* **13**, 461–469 (2015).
54. J. Mercer, Viral apoptotic mimicry party: P.S. bring your own gas6. *Cell Host Microbe* **9**, 255–257 (2011).
55. M. L. Husby *et al.*, Phosphatidylserine clustering by the Ebola virus matrix protein is a critical step in viral budding. *EMBO Rep.* **23**, e51709 (2022).
56. A. S. Richard *et al.*, Virion-associated phosphatidylethanolamine promotes TIM1-mediated infection by Ebola, dengue, and West Nile viruses. *Proc. Natl. Acad. Sci. U.S.A.* **112**, 14682–14687 (2015).
57. J. M. Thomas, P. E. Thorpe, Protective effect of anti-phosphatidylserine antibody in a guinea pig model of advanced hemorrhagic arenavirus infection. *Open Microbiol. J.* **11**, 303–315 (2017).
58. G. K. Atkin-Smith *et al.*, Monocyte apoptotic bodies are vehicles for influenza A virus propagation. *Commun. Biol.* **3**, 223 (2020).
59. G. Franzoni *et al.*, Characterization of the interaction of African swine fever virus with monocytes and derived macrophage subsets. *Vet. Microbiol.* **198**, 88–98 (2017).
60. G. Lemke, How macrophages deal with death. *Nat. Rev. Immunol.* **19**, 539–549 (2019).
61. S. P. Hart, I. Dransfield, A. G. Rossi, Phagocytosis of apoptotic cells. *Methods* **44**, 280–285 (2008).